J. Fluid Mech. (1968), *vol.* 33, *part* 1, *pp.* 38–63
Printed in Great Britain

On the singular points in the laminar two-dimensional near wake flow field

By SHELDON WEINBAUM

Department of Mechanical Engineering,
The City College of The City University, New York, New York 10031

(Received 17 April 1967 and in revised form 22 December 1967)

It is shown that useful information concerning the flow in the neighbourhood of the various separation and stagnation points in the laminar near wake of a blunt-based two-dimensional wedge can be learned from the locally valid Stokes type series solutions to the incompressible Navier–Stokes vorticity equation derived previously by Dean & Montagnon (1949) and Moffatt (1964). This theory, which is in qualitative agreement with the experiments of Hama (1967) and Donaldson (1967), shows that the flow separates from the base of a blunt-based body and not from its trailing edge. The series solution for the two-dimensional stagnation point is treated in detail and compared with Howarth's (1934) numerical solution in order to study the convergence and conditions for completeness of the Stokes type series solution. Finally, the wake rear stagnation point is examined to provide insight into the problem of wake closure.

1. Introduction

The detailed description of the laminar, hypersonic, near wake behind a blunt-based body has proved to be one of the most difficult and important problems in modern fluid mechanics both from a mathematical and conceptual viewpoint. One aspect of this problem which has been the subject of continuing interest is the detailed understanding of the local phenomena associated with the three elliptic singular points: the separation point, the base stagnation point and the rear stagnation point that form the vertices of the entrained flow region (see figure 1). Of particular interest is the local behaviour whereby the flow first separates at a blunt-based trailing edge and then reattaches further downstream to form a closed wake. It is the theme of the present paper to show that insight into both these phenomena can be obtained from local Stokes type series solutions.

Some of the recent developments relating to the above problem areas shall now be briefly reviewed. We start with separation point flow. The series of experiments just completed at the Jet Propulsion Laboratory by Hama (1967) and the corroborating experimental results of Donaldson (1967) have pointed to a number of anomalies in the theory developed by Weinbaum (1966*b*) and Weiss & Weinbaum (1966) for the expansion and separation process that occurs at a blunt-based trailing edge. These authors adopt an inviscid rotational model

for the supersonic portion of the expanding boundary-layer flow. It is assumed that the origin of the expansion fan is positioned at the corner and that separation occurs at the trailing edge. Rotational characteristic calculations based on this model are then performed to study the interaction of the expanding boundary layer with an essentially constant pressure base region. Such a model predicts

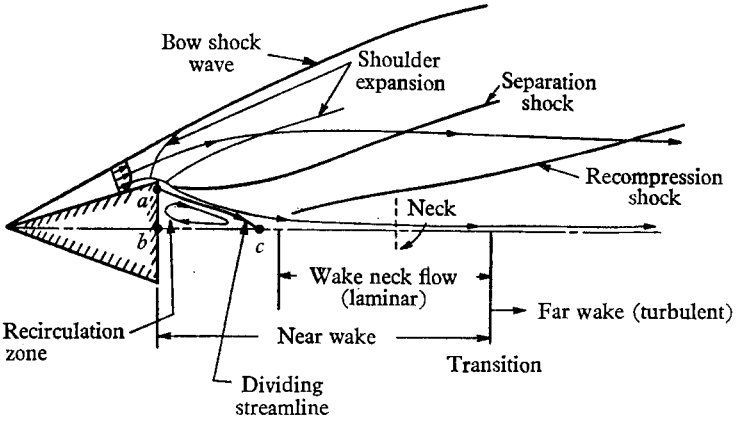

FIGURE 1. Schematic diagram of near wake flow field. *a*, separation point. *b*, base stagnation point. *c*, rear stagnation point.

that the reflected waves from the constant pressure region will coalesce typically 5 to 10 boundary-layer thicknesses downstream of the corner to form the well-documented 'lip' or separation shock wave (see figures 1 and 2). Hama's detailed experiments indicated that this shock formation distance is an order of magnitude too large; his measurements show this distance is typically less than a boundary-layer thickness, and that the foot of the shock wave appears to be located beneath the corner and adjacent to the base wall (see figure 2, plate 1). Moreover, the accompanying static pressure measurements show that the wall pressure does not fall monotonically across the corner, as most investigators have assumed till now, but reaches a minimum at some distance small compared to a boundary-layer thickness, just prior to or after the corner. The pressure along the rear wall then increases sharply with distance from the corner and asymptotically approaches the base pressure value from below after a distance of the order of several boundary-layer thicknesses. Except for the basic wave mechanism, which is responsible for the lip shock, all these observations are at variance with the inviscid model described above. To explain these discrepancies it was felt that more had to be learned about the details of the viscous separation process and, in particular, about the manner in which pressure signals from the low-pressure base region are communicated across the corner. Three characteristic length scales are present; an inertial–viscous interaction distance, the boundary-layer thickness; a pressure–viscous interaction distance, the Stokes radius; and a finer scale in which the near equilibrium continuum description provided by Navier–Stokes viscous stresses is no longer valid, the Knudsen radius. A qualitative picture of the pressure behaviour on the first length scale is available from

Hama's measurements, which were taken to within approximately half a boundary-layer thickness of the corner. On the Stokes length scale one would anticipate the velocity to be continuous everywhere, but the pressure and density to be singular at the origin to accommodate the rapid changes in these variables that are taking place on the Knudsen length scale. In the Stokes region, where the lowest order force balance is between pressure and viscous forces, the effect of compressibility on the viscous terms in the momentum equation enters through the thermal dependence of the viscosity coefficient, which is a higher order effect if a zeroth order temperature slip does not occur at the wall, and indirectly through the density dependence of the continuity equation. Thus, if the velocity field and streamline patterns for a compressible and incompressible flow are qualitatively similar in the viscous region, their pressure distributions should likewise be qualitatively similar in this region. The comparison of the results of the incompressible theory with Hama's experimental data appears to bear out this conjecture.† The incompressible analysis is also of interest in itself. There has been some controversy as to whether or not the wall shear stress vanishes at a blunt-based trailing edge for an incompressible fluid (Viviand & Berger 1965).

For the other two singular points, the base and rear stagnation points, the incompressible assumption is not as severe an approximation. For all three singular regions we then use a Stokes type series expansion of the incompressible Navier–Stokes vorticity equation. The vorticity formulation is chosen since the flow variable whose behaviour is least well understood, the pressure, does not appear explicitly. When the singular point is part of a solid boundary, the leading terms of the series are the slow motion eigenfunctions derived by Dean & Montagnon (1949) and extended by Moffatt (1964) for 'creep' flows interior and exterior to a sharp dihedral angle. A number of investigators have also attempted to construct iterative solutions to the non-linear Navier–Stokes equation starting with the Stokes type solution. For example, Carrier & Lin (1948) and, more recently, Lugt & Schwiderski (1965) have employed this technique to describe the leading edge flow past a flat plate. The latter authors suggest that integrals of the non-linear Navier–Stokes equation for the flow in the vicinity of a dihedral angle can, in general, be constructed in an exact and linear manner in terms of the fundamental slow motion solutions. The present analysis shows this suggestion to be false. Additional insight into this question can be had by studying the properties of the Stokes type series solution about a two-dimensional stagnation point. Lugt & Schwiderski also derive the first few terms of this series solution, but they do not discuss its physical significance, rate of convergence or conditions for completeness. When each of the terms is carefully analysed to examine the detailed coupling between viscous and inertial effects and the series solution compared with Howarth's (1934) exact numerical solution, one finds that the pressure field is comprised of two fundamentally different components, one associated with the viscous stresses produced at the boundary and the second with the external flow. Only for rather special flow geometries is the

† Roache (1967) has just confirmed the qualitative similarity between the behaviour of the incompressible and compressible flows in his numerical solution of the incompressible and compressible flow in the vicinity of a sharp corner.

Stokes type series sufficiently general to describe the motion due to the latter component. These results are closely related to the theory of inner and outer expansions. Harper (1963) has investigated the nature of the viscous and inviscid flow regions in the vicinity of the base stagnation point. He has shown that even though the entrained flow has vorticity, the inviscid flow in the immediate vicinity of the stagnation point boundary layer is nearly irrotational. Thus, the classical two-dimensional stagnation point analysis is also valid locally about the base stagnation point.

One question of general interest that may be of special importance with regard to the rear stagnation point is whether the constraints imposed by the three singular points affect the over-all motion, or are these constraints higher order effects that only require the flow to adjust locally. For real fluids satisfying viscous boundary conditions, this question is unanswered; for ideal inviscid flows, the former is true. It is well known, for example, that the location of the separation point on a body uniquely determines the circulation about the body and hence influences the entire flow pattern. The classical illustration is the Kutta condition in inviscid airfoil lifting theory. The fact that separation is observed to occur at or very near the trailing edge of a sharp-edged airfoil at small angles of attack in a real fluid suggests that there is a close relationship between the viscous and inviscid separation conditions. This conjecture is supported by the present viscous analysis. This theory shows that a large asymmetric freestream component is needed to displace the trailing edge separation point more than a Stokes radius from a sharp trailing edge. It has been suggested by Weinbaum (1967) that the rear stagnation point may play a role in the wake that is similar to the Kutta condition in inviscid airfoil theory. First, the rear stagnation point represents a point of velocity coupling between the retardation of velocity of the flow along the dividing streamline prior to stagnation and the initial growth of velocity of the flow that is redirected back toward the base. This local flow, therefore, may be important in determining the circulation about and hence vorticity within the entrained flow region. Secondly, the mechanism of wake closure could possibly provide a uniqueness constraint for the circulation if there were some invariant behaviour characteristic of the local stagnation point flow that was independent of the external flow.†

In general, the arbitrary constant coefficients that appear in the leading terms of a locally valid series solution depend upon the gross features of the external flow, such as its flow direction and level of energy input. Thus, if a unique closure condition is to exist it should be independent of these constant coefficients which characterize the gross features of the external flow. While the Stokes type series solutions considered herein do show the existence of such a condition, these solutions cannot be used to provide insight into how this condition is to be related to the overall motion. The latter involves the difficult unsolved problem of matching inner Stokes flows with outer inertial flows.

† Such a constraint would not be inconsistent with the so called 'throat constraint' of Crocco & Lees (1952) theory which is derived from linear momentum considerations.

2. General theory

The governing equations which shall be used to describe qualitatively the various stagnation and separation point flow phenomena are the incompressible Navier–Stokes equations. One introduces the following dimensionless variables:

$$u = \frac{u^*}{u_\infty}, \quad v = \frac{v^*}{u_\infty}, \quad p = \frac{p^*}{\rho_\infty u_\infty^2}, \quad r = \frac{r^*}{L}, \quad 1 = \frac{\rho^*}{\rho_\infty} \tag{2.1}$$

(dimensional quantities are shown with asterisks), and chooses $L = \nu_\infty/u_\infty$ as the characteristic reference length. This corresponds to setting $Re_\infty = u_\infty L/\nu_\infty = 1$; thus, $r = 1$ is representative of the dimensions of a Stokes type slow flow region about the singular point. The dimensionless conservation equations are:

$$uu_r + \frac{v}{r}u_\theta - \frac{v^2}{r} = -p_r - \frac{1}{r}\frac{\partial}{\partial\theta}\left(v_r + \frac{v}{r} - \frac{1}{r}u_\theta\right), \tag{2.2}$$

$$uv_r + \frac{vv_\theta}{r} + \frac{uv}{r} = -\frac{1}{r}p_\theta + \frac{\partial}{\partial r}\left(v_r + \frac{v}{r} - \frac{1}{r}u_\theta\right), \tag{2.3}$$

$$\frac{\partial(ur)}{\partial r} + \frac{\partial v}{\partial\theta} = 0. \tag{2.4}$$

Here $\bar{V} = u\bar{r} + v\bar{\theta}$, where the polar co-ordinates (r, θ) are the most convenient co-ordinates for satisfying the boundary conditions in the problems of interest. One eliminates p between (2.2) and (2.3), to reduce the number of dependent variables, and introduces the two-dimensional stream function ψ:

$$u = \frac{1}{r}\psi_\theta, \quad v = -\psi_r. \tag{2.5}$$

This is one convenient way of reducing (2.2), (2.3) and (2.4) to one equation in a single unknown function ψ:

$$\left.\begin{aligned} -\left[\psi_r\frac{\partial}{\partial\theta} - \psi_\theta\frac{\partial}{\partial r}\right]\nabla^2\psi &= r\nabla^2\nabla^2\psi, \\ \nabla^2 &= \frac{\partial^2}{\partial r^2} + \frac{1}{r}\frac{\partial}{\partial r} + \frac{1}{r^2}\frac{\partial^2}{\partial\theta^2}. \end{aligned}\right\} \tag{2.6}$$

Note, we have not divided through by r, since we shall want to examine the limiting behaviour of each of the terms in (2.2), (2.3) and (2.6) as $r \to 0$.

Let us assume, for the moment, that ψ behaves as r^m, m not necessarily integer, as $r \to 0$. The non-linear term in (2.6) and the acceleration terms in (2.2) and (2.3) behave as r^{2m-3} as $r \to 0$, while the linear viscous terms in (2.2), (2.3) and (2.6) behave as r^{m-3} as $r \to 0$. Thus, the requirement that the viscous terms dominate and that the flow exhibit a Stokes type slow flow behaviour in some small neighbourhood of $r = 0$ is that $m > 0$. This requirement, however, is too weak since physical considerations require that the velocity be continuous across the corner. From (2.5), this last condition is satisfied if $m \geqslant 1$, where the inequality sign applies for a solid boundary if one allows no slip. The fact that the

shear stress and the pressure are singular at $r = 0$ when $m < 2$ should not be a matter of serious concern. Pointed edges with zero bluntness are a mathematical idealization that is not found in nature, and it is not surprising that within the framework of the Navier–Stokes equation, where the linear stress-strain relationship describes only small departures from equilibrium, such edges will produce an infinite shear stress on a fluid element at $r = 0$ if no slip is allowed. The physically meaningful limitation is that the integrated shear or the viscous force acting at the sharp edge be bounded. Since the latter behaves as r^{m-1}, we again require that $m > 1$.

Thus, the leading term $\psi^{(0)}$ of an expansion for ψ about a sharp edge should exhibit a Stokes type flow behaviour, hence satisfy the biharmonic equation,

$$\psi^{(0)}_{rrrr} + \frac{2}{r}\psi^{(0)}_{rrr} - \frac{1}{r^2}\psi^{(0)}_{rr} + \frac{1}{r^3}\psi^{(0)}_{r} + \frac{4}{r^4}\psi^{(0)}_{\theta\theta} - \frac{2}{r^3}\psi^{(0)}_{r\theta\theta} + \frac{2}{r^2}\psi^{(0)}_{rr\theta\theta} + \frac{1}{r^4}\psi^{(0)}_{\theta\theta\theta\theta} = 0, \tag{2.7}$$

whenever $\psi^{(0)} \to 0$ more slowly than r as $r \to 0$. There are numerous solutions to the biharmonic equation in polar co-ordinates; however, as Dean & Montagnon (1949), Moffatt (1964), and Lugt & Schwiderski (1965) have previously shown, the only solutions which satisfy the no slip condition along a $\theta =$ constant line are of the form,

$$\psi^{(0)} = r^m f_1(\theta), \tag{2.8}$$

$$f_1 = A_1 \sin m\theta + A_2 \sin[(m-2)\theta] + A_3 \cos m\theta + A_4 \cos[(m-2)\theta] \quad (m \neq 2), \tag{2.9a}$$

$$f_1 = A_1 \sin 2\theta + A_2\theta + A_3 \cos 2\theta + A_4 \quad (m = 2), \tag{2.9b}$$

where m is any number, real or complex, and the constants A_i must be chosen so as to satisfy all boundary and matching conditions. In the present study, we shall be concerned only with the solutions for m real since they describe the flow near sharp edged obstacles. The solutions for m complex represent viscous vortices in a sharp corner (Moffatt 1964). Since (2.7) is linear, any number of solutions can be superposed provided each satisfies the boundary conditions.

3. Slow motion eigenfunctions

For a solid boundary, let the wall angle θ_0 be measured relative to the x-axis or angle bisector as shown in figure 3. $\theta_0 = \frac{1}{2}\pi, \frac{3}{4}\pi, \pi$ then represents the base stagnation point, the 90-degree blunt-based trailing edge, and the flat plate leading or trailing edge in that order. The zero slip boundary condition, $u = v = 0$ at $\theta = \pm\theta_0$, requires that

$$f_1(\pm\theta_0) = 0, \quad f_1'(\pm\theta_0) = 0. \tag{3.1}$$

For a symmetric flow, the stream function is antisymmetric about the plane $y = 0$. $A_3 = A_4 = 0$, and if A_1 and A_2 are to have a non-trivial solution and satisfy the boundary-conditions equation (3.1),

$$m \sin 2\theta_0 - 2(\sin m\theta_0)\cos[(m-2)\theta_0] = 0 \quad (m \neq 2). \tag{3.2a}$$

The corresponding result for an antisymmetric flow ($A_1 = A_2 = 0, A_3$ and $A_4 \neq 0$) is

$$m \sin 2\theta_0 + 2(\cos m\theta_0)\sin[(m-2)\theta_0] = 0 \quad (m \neq 2). \tag{3.2b}$$

The case $m = 2$ for (3.2a) is obtainable by differentiating with respect to m.

The solutions to (3.2*a*) and (3.2*b*) are shown in figure 4 and table 1. These numerical results, which were obtained independently by the author, are the same as those reported by Lugt & Schwiderski (1965); however, our use and interpretation of these results will differ. First one notes that, although there is

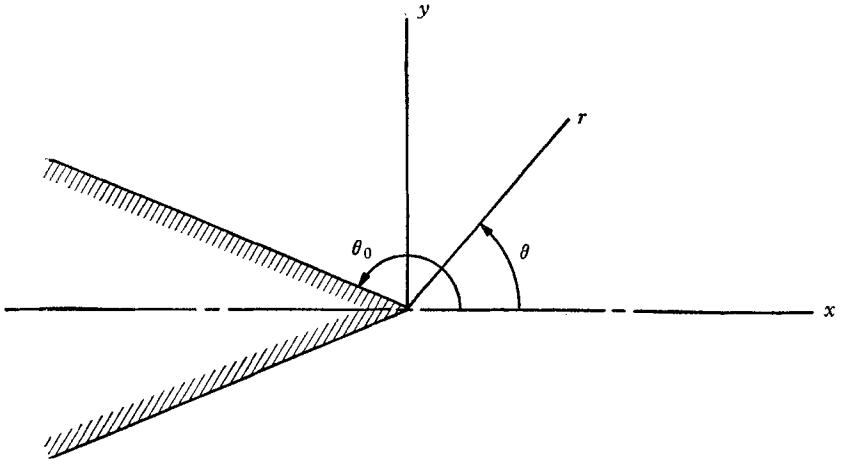

FIGURE 3. Schematic diagram of dihedral angle.

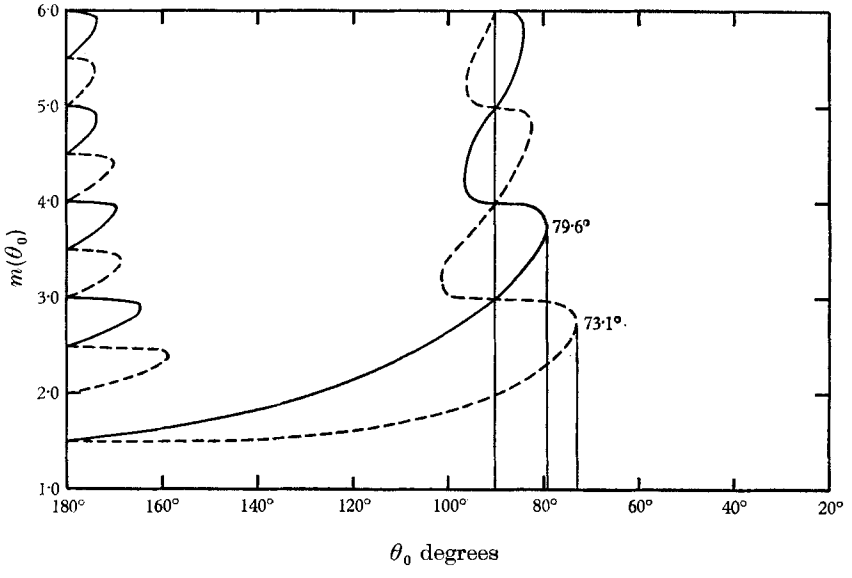

FIGURE 4. Roots of equation (3.2) for power $m = m(\theta_0)$ of wedge singularity. ——, equation (3.2*a*), symmetric flow; – – –, equation (3.2*b*), antisymmetric flow.

an infinite multiplicity of symmetric and antisymmetric eigenvalues for both the $\theta_0 = \frac{1}{2}\pi$ and $\theta_0 = \pi$ cases, there is only one symmetric and one antisymmetric solution curve that connects these two cases when m is real. Intuitively, one would expect that the flat plate is not an isolated case but rather the limiting case of a

flat wall collapsed into a plane. Thus, the streamline pattern in the vicinity of the edge should not change abruptly as one varies the dihedral angle in the range $\frac{1}{2}\pi \leqslant \theta_0 \leqslant \pi$. This is only possible if one chooses lowest order eigenvalues for m

Symmetric roots, equation (3.2a)

θ_0	m	θ_0	m	θ_0	m
79·6	3·746	110	2·360	145	1·785
80	3·661	115	2·249	150	1·731
85	3·254	120	2·149	155	1·683
90	3·000	125	2·061	160	1·638
95	2·800	130	1·981	165	1·598
100	2·631	135	1·909	170	1·562
105	2·480	140	1·844	175	1·530
				180	1·500

Antisymmetric roots, equation (3.2b)

θ_0	m	θ_0	m	θ_0	m
73·1	2·748	110	1·697	150	1·512
75	2·534	115	1·652	155	1·507
80	2·288	120	1·616	160	1·503
85	2·125	125	1·586	165	1·501
90	2·000	130	1·563	170	1·500
95	1·900	135	1·544	175	1·500
100	1·819	140	1·530	180	1·500
105	1·752	145	1·520		

TABLE 1. Roots of equation (3.2), $m = m(\theta_0)$

that are continuous in the range $\frac{1}{2}\pi \leqslant \theta_0 \leqslant \pi$. Since one can show indisputably, as we shall in §5, that $m = 3$ when $\theta_0 = \frac{1}{2}\pi$, m is $\frac{3}{2}$ for a flat plate as Carrier & Lin predicted. The flat plate solution suggested by Lugt & Schwiderski, which is based on the eigenvalues $m = 3$ and $\frac{7}{2}$, is probably not physically meaningful. One notes from figure 4 that the eigenvalue curves through these points do not permit solutions of the same general character as the flat plate solution for a wide range of wedge angles intermediate between the $\theta_0 = \frac{1}{2}\pi$ and π cases.

Two other points are of interest in figure 4: (a) the significance of the higher order solutions for m, and (b) the absence of any real solutions for m for $\theta_0 < 79{\cdot}6$ and 73·1 degrees for symmetric and antisymmetric flows, respectively. In reference to (a), the complete series solution for the $\theta_0 = \frac{1}{2}\pi$ case in §5 shows that the lowest order eigensolution for $\psi^{(0)}$ describes only the local pressure field due to the dilation and rotational distortion of the fluid element produced by the fluid motion adjacent to the boundary. The inertial motion of the fluid outside the boundary layer also produces a pressure field that is transmitted through the boundary layer into the viscous region which must be balanced by viscous stresses. This latter pressure–viscous force balance must also satisfy the viscous zero slip boundary conditions. For the $\theta_0 = \frac{1}{2}\pi$ case, this force balance is described by the next higher order eigensolution for $\psi^{(0)}$. For other wedge angles, higher order eigensolutions corresponding to m real do not always exist (see figure 4); and even

where they do exist, there is no assurance that any combination of these solutions is sufficiently general to describe the effect in the viscous region of the non-linear inertial pressure field imposed by the external flow. Point (*b*) is treated by Moffatt. As mentioned earlier, complex solutions for m do exist for these angles. These solutions describe a series of decaying viscous eddies in a sharp corner.

The leading terms of the series that describe the Stokes type region for the flow external to a dihedral angle are from (2.9*a*), (3.1), (3.2*a*) and (3.2*b*):

$$\psi^{(0)} = A_1 r^{m_1}\left[\cos m_1\theta - \frac{\cos m_1\theta_0}{\cos[(m_1-2)\theta_0]}\cos[(m_1-2)\theta]\right] + A_2 r^{m_2}\left[\sin m_2\theta - \frac{\sin m_2\theta_0}{\sin[(m_2-2)\theta_0]}\sin[(m_2-2)\theta]\right] + O(r^{2m_1}), \quad (3.3)$$

where the arbitrary constants A_1 and A_2 have been redefined. The eigenvalues m_1 and m_2 correspond to the antisymmetric and symmetric flow components, respectively. Well-known special cases of (3.3) are the Carrier & Lin flat plate leading edge solution; $A_1 = 0$, $A_2 \neq 0$, $m_2 = \frac{3}{2}$, and the Oswatitsch solution for the separation point flow at a solid boundary; A_1 and $A_2 \neq 0$, $m_1 = m_2 = 3$. Note that there appears to be no distinction between the solutions for a leading or trailing edge other than the magnitude of the constants and the fact that the sign of $\psi^{(0)}$ has to be adjusted to provide the proper flow direction. The implication is that the flow right near the leading or trailing edge is independent of the details of the energy input or driving mechanism at distances large compared to the Stokes radius.

4. Higher order solutions

In this section, we shall briefly outline a method for obtaining the higher order terms in a Stokes type series. We emphasize that the difficult mathematical problem is not to construct the series but to determine the unknown constant coefficients that appear and to show that the series is complete. These points shall be explored further in the next section for the case $\theta_0 = \frac{1}{2}\pi$. The generating function for the Stokes series is of the form

$$\psi^{(0)} = \sum_{j=1}^{\infty} r^{m_j} f_j^{(0)}(\theta), \quad (4.1)$$

where the m_j represent the various eigenvalues of (3.2) and N is the total number of terms required to describe the complete pressure–viscous balance in the Stokes region, provided terms of the type (4.1) are suitable for describing the pressure field characteristic of the external flow. One need not include all the m_j, e.g. the case $\theta_0 = \frac{1}{2}\pi$ has an infinite number of eigenvalues, $m_j = 3, 4, 5, \ldots$, etc.; however, only the terms for $m_j = 3$ and 4 are required to construct the series.

The series expansion takes the form (compare Carrier & Lin (1948) and Lugt & Schwiderski (1965))

$$\psi = \psi^{(0)} + \psi^{(1)} + \psi^{(2)} + \ldots, \quad (4.2)$$

where

$$\left.\begin{aligned} \nabla^2\nabla^2\psi^{(0)} &= 0, \\ \nabla^2\nabla^2\psi^{(1)} &= L_1(\psi^{(0)}), \\ \nabla^2\nabla^2\psi^{(2)} &= L_2(\psi^{(0)}, \psi^{(1)}), \text{etc.}, \end{aligned}\right\} \quad (4.3)$$

and the L_i are the appropriate non-linear convective operators obtained from the left-hand side of (2.6).

The mechanics of solving the linear system of equations (4.3) is straightforward, and is described in Lugt & Schwiderski (1965) and Weinbaum (1966*a*). The solution for $\psi^{(1)}$ contains $\frac{1}{2}N(N+1)$ terms of the form

$$\psi^{(1)}_{jk} = r^{(m_j+m_k)} f^{(1)}_{jk}(\theta) \quad (j=1,2,\ldots,N; k=1,2,\ldots,-N),$$

one for each power of r form that occurs in the inhomogeneous part $L_1(\psi^{(0)})$. Each $f^{(1)}_{jk}(\theta)$ must obey the wall boundary condition

$$f^{(1)}_{jk}(\pm\theta_0) = f^{(1)\prime}_{jk}(\pm\theta_0) = 0, \tag{4.4}$$

if there is to be no slip at the body. Except for the special cases $\theta_0 = \frac{1}{2}\pi$ and π, the solutions to the reduced equations for the $f^{(1)}_{jk}$ do not vanish at the boundaries. The homogeneous and particular integrals can, therefore, be added, and the constants in the homogeneous integral determined so as to satisfy the boundary conditions (4.4). These constants depend only on the wall angle θ_0 and the constant coefficients A_i of the fundamental slow motion eigenfunctions. The series development can be continued in a like manner to find $\psi^{(2)}$, $\psi^{(3)}$, etc., and all the constants in the higher order terms related to the A_i. When $\theta_0 = \pi$ and $m_1 = \frac{3}{2}$ the particular solution contains secular terms which when added to the integral of the reduced equation do not satisfy the zero-slip condition. A series based on powers of r alone is not sufficiently general and one must extend the series to include the so-called 'associated separable slow-motion solutions of order n' (see Lugt & Schwiderski 1965)

$$\psi^n_{m_j} = \frac{\partial^n}{\partial m_j^n} r^{m_j} f_j(\theta). \tag{4.5}$$

These solutions, which also obey the biharmonic equation, balance the contributions of the secular terms at the wall and thereby enable the zero-slip condition to be satisfied. The other special case, $\theta_0 = \frac{1}{2}\pi$, is discussed in the next section.

5. The base stagnation point

The theory developed in §§2–4 will now be applied to the case $\theta_0 = \frac{1}{2}\pi$ and the results compared with Howarth's (1934) exact numerical solution of the governing differential equations. The mechanics of deriving the first few terms of this series solution is presented in the Lugt & Schwiderski paper. These authors do not explore these results further. The series expansion can also be obtained from the appropriate Falkner–Skan boundary-layer equation. The primary object here is not to derive additional terms in this series but to (i) investigate under what conditions a Stokes type series solution about a separation or stagnation point will converge to the correct solution in the flow region where inertial effects are important, (ii) study the rapidity of convergence of such a series, and (iii) examine the term-by-term coupling between the viscous and inviscid flow regions.

It is well known that for an incompressible two-dimensional stagnation point flow the boundary-layer thickness is constant, since the thinning of the boundary

layer due to the acceleration of the fluid by the pressure field is just balanced by the thickening of the boundary layer due to diffusion. Because of this, the displaced external potential flow ψ_e is also that of a plane flow

$$\psi_e = -\beta xy, \tag{5.1}$$

where β is an arbitrary positive constant. We normalize the equations with respect to β by stretching the distance co-ordinates:

$$\xi = (\beta x)^{\frac{1}{2}}, \quad \eta = (\beta y)^{\frac{1}{2}}, \quad R = (\beta r)^{\frac{1}{2}}. \tag{5.2}$$

Because of the planar property of the viscous flow that $u_x = F(x)$ one can show readily that the components of the Navier–Stokes momentum equation parallel and perpendicular to the boundary reduce to

$$\frac{1}{\beta} p_\eta = -\psi_{\xi\xi\xi} + \psi_\eta \psi_{\xi\xi} - \psi_\xi \psi_{\xi\eta} = -\eta, \tag{5.3}$$

$$\frac{1}{\beta} p_\xi = -\psi_\eta \psi_{\eta\xi} + \psi_{\eta\xi\xi}, \tag{5.4}$$

in that order, where $u_x = \psi_y$ and $u_y = -\psi_x$. The vorticity equation (2.6) is unchanged except that R appears in place of r.

From (3.3) and figure 4, the two leading terms of a Stokes type series which correspond to the two lowest order eigenvalues $m_j = 3$ and 4 are

$$\begin{aligned} \psi^{(0)} &= A_1 R^3(\sin\theta + \sin 3\theta) + A_2 R^4(\sin 4\theta + 2\sin 2\theta) \\ &= 4A_1\eta\xi^2 + 8A_2\eta\xi^3. \end{aligned} \tag{5.5}$$

The important observation is that these two terms play a different role in the generation of the series expansion and have a different physical significance. The first term provides the dominant contribution to the normal pressure gradient in the viscous region, equation (5.4), but plays no role in balancing the pressure gradient in the η direction, $p_\eta = -\beta\eta$, established by the inviscid motion of the external flow. On the other hand, the second term provides a higher order contribution to the normal pressure gradient, but is the key term coupling the inertial motion of the outer flow with the inner viscous region. According to boundary-layer theory, the external pressure gradient is transmitted through the viscous layer to the wall where it is balanced by the shear stress gradient $(\partial/\partial\eta)(\partial u_y/\partial\xi)$ at the boundary. Thus, if the A_2 term is to balance the pressure gradient produced by the external flow in the limit as $R \to 0$, then from (5.3), $A_2 = \frac{1}{48}$. In contrast, the pressure–viscous balance attributed to the A_1 term is due to the dilation and rotational deformation of the fluid element near the boundary caused by the motion of the fluid element *per se*. The amplitude of this viscous deformation is related to the outer flow by the value of the constant A_1. No further terms are required to describe the complete pressure–viscous force balance near $R = 0$. The term in R^5 in the Lugt & Schwiderski solution should not be present.

Following the procedure outlined in §4, the author derived the first eleven terms of the series solution, using just the two Stokes terms, equation (5.5), as generating functions. The detailed solution is presented in Weinbaum (1966*a*).

All the constants of the higher order terms can be related to A_1. Letting $\alpha = 4A_1$, one obtains

$$\psi = -\eta\left[\alpha\xi^2 - \frac{1}{6}\xi^3 + \frac{\alpha^2}{30}\xi^5 - \frac{\alpha}{180}\xi^6 + \frac{1}{2520}\xi^7 - \frac{\alpha^3}{5040}\xi^8 + \frac{\alpha^2}{22{,}680}\xi^9 - \frac{\alpha}{113{,}400}\xi^{10} + \left(\frac{\alpha^4}{92{,}400} + \frac{1}{2{,}494{,}800}\right)\xi^{11} - \frac{181\alpha^3}{(5040)(11{,}880)}\xi^{12} + \frac{41\alpha^2}{(11{,}340)(17{,}160)}\xi^{13} + \ldots\right]. \quad (5.6)$$

The series in brackets in (5.6) is just Howarth's function ϕ. α, the only remaining undetermined constant, can be evaluated by either matching the series solution with Howarth's value for the shear stress at the wall, in which case $\alpha = 0{\cdot}6162938$,

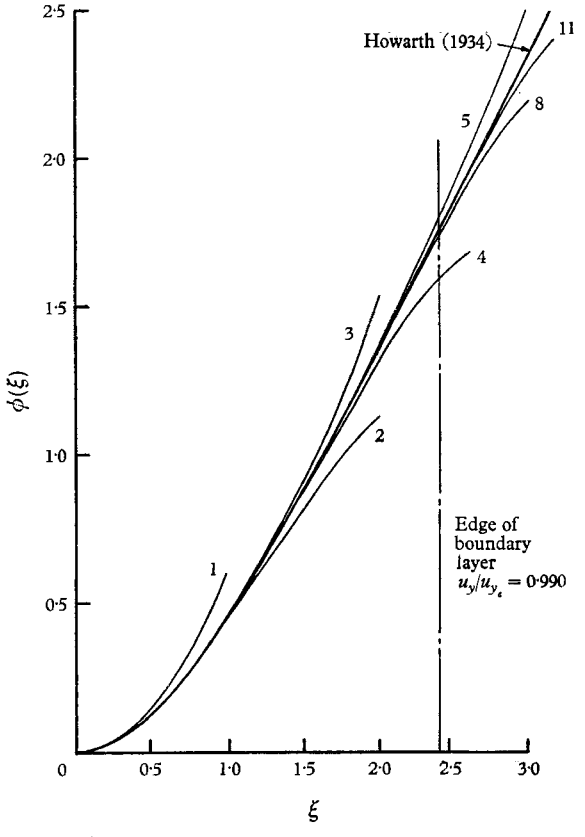

FIGURE 5. Convergence of series solution for ϕ (ξ), $\theta_0 = \frac{1}{2}\pi$ case.

or by choosing α such that ϕ exhibits the proper behaviour at the edge of the boundary layer, i.e. $\phi_\xi \to 1$; the series, of course, must contain enough terms to describe adequately this flow region. In figure 5 and in table 2 we have compared Howarth's solution and the series solution for ϕ, having truncated the latter after 1, 2, 3, 4, 5, 8 and 11 terms, respectively. The third and fifth terms of the series represent the first inertial corrections to the A_1 and A_2 terms, and the fourth term the first inertial coupling of the two pressure effects. As shown, the five-

term series truncation is accurate to within about 1 % up to $\xi = 2{\cdot}4$, at which point $u_y/u_{y_e} = 0{\cdot}990$.

		$\phi(\xi)$ series solution Number of terms						
ξ	$\phi(\xi)$ Howarth (1934) exact solution	1	2	3	4	5	8	11
0	0·0	0·0	0·0	0·0	0·0	0·0	0·0	0·0
0·1	0·0060	0·00616	0·00600	0·00600	0·00600	0·00600	0·00600	0·00600
0·2	0·0233	0·02465	0·02332	0·02332	0·02332	0·02332	0·02332	0·02332
0·4	0·0881	0·09861	0·08794	0·08807	0·08806	0·08806	0·08806	0·08806
0·6	0·1867	0·22187	0·18587	0·18685	0·18669	0·18670	0·18670	0·18670
0·8	0·3124	0·39443	0·30909	0·31324	0·31235	0·31243	0·31242	0·31242
1·0	0·4592	0·61629	0·44963	0·46229	0·45886	0·45926	0·45923	0·45923
1·2	0·6220	0·88746	0·59946	0·63097	0·62074	0·62217	0·62202	0·62203
1·4	0·7967	1·20794	0·75060	0·81869	0·79291	0·79710	0·79660	0·79665
1·6	0·9798	1·57771	0·89505	1·02780	0·97036	0·98101	0·97957	0·97975
1·8	1·1689	1·99679	1·02479	1·26402	1·14757	1·17186	1·16813	1·16874
2·0	1·3620	2·46518	1·13184	1·53698	1·31785	1·36865	1·35977	1·36154
2·2	1·5578	2·98286	1·20820	1·86068	1·47248	1·57146	1·55176	1·55639
2·4	1·7553	3·54985	1·24585	2·25397	1·59966	1·78166	1·74032	1·75135
2·6	1·9538	4·16615	1·23681	2·74107	1·68338	2·00211	1·91933	1·94367
2·8	2·1530	4·83174	1·17308	3·35201	1·70209	2·23752	2·07824	2·12868
3·0	2·3526	5·54664	1·04664	4·12317	1·62718	2·49504	2·19903	2·29815

TABLE 2. Comparison of series and exact solution for $\phi(\xi)$ for $\theta_0 = \frac{1}{2}\pi$ case

It is evident from the foregoing results and discussion for the $\theta_0 = \frac{1}{2}\pi$ case that for the general case one cannot construct in an exact and linear manner integrals to the non-linear Navier–Stokes equation which are based on fundamental slow-motion solutions. A unique description of the Stokes flow region involves two distinctly different pressure–viscous force balances, and a Stokes type expansion will not be complete unless both force balances are taken in account. While one can write down for any convex angle the leading symmetric and antisymmetric terms of the series which describe the local pressure field established by the viscous stresses in the vicinity of the singularity, this is not true for the lowest order terms which describe the inertial component of the pressure field that is felt through the boundary layer. One notes from figure 4 that there is a wide range of angles $100 < \theta_0 < 160$ degrees for which no such slow motion eigenfunctions exist with m real. Though, as Moffatt (1964) and Lugt & Schwiderski (1965) show, complex eigenfunctions do exist for these angles, the pressure fields characteristic of these eddy type solutions are not representative of the inertial motion one would expect for the flow past a sharp corner. In general, the displacement effect of the dissipative mechanisms in the vicinity of the singular point will cause a significant distortion of the actual body shape as far as the outer inviscid flow is concerned. Thus, unlike the $\theta_0 = \frac{1}{2}\pi$ case, where the displaced external flow is known, equation (5.1), and the inertial pressure field specified, the inertial motion in the general case is not known in advance and has to be determined as part of the solution. This difficult problem of matching inner Stokes flows with disturbed outer inertial flows has still to be solved.

6. The blunt-based trailing edge

Existing viscous layer theories, e.g. Denison & Baum (1963) and Kubota & Dewey (1964), for development of the separated boundary flow on a blunt-based body are in the large part extensions of Goldstein's (1930) zero-thickness flat-plate solution. These extensions are an inadequate representation of the flow near the separation point of a blunt-based body for they invoke the following simplifying assumptions: (i) all upstream influence can be neglected; the boundary-layer flow is both parallel to the wall and has a Blasius profile at the separation point. (ii) Normal momentum need not be conserved; the boundary-layer equations of motion are used locally. (iii) The zero slip boundary condition imposed by the rear wall can be violated; this is a critical oversimplification since there can be no angular momentum Reynolds number effect for the base region if one neglects the resisting torque at the rear wall. Also, the initial growth of velocity along the dividing streamline should be significantly inhibited by the presence of the rear wall. (iv) The pressure is uniform throughout the entire flow; this is a serious violation in both the slow flow region surrounding the separation point and in the inertial region where lowest order pressure gradients are produced by the corner expansion. (v) The inclination angle of the dividing streamline can be ignored in the mixing process that takes place downstream of the separation point; this is a poor approximation since the shearing stress induced on the rear wall, hence the resisting torque exerted on the recirculating flow, is very sensitive to the separation angle of the dividing streamline. This angle can be as large as 50 degrees in some problems of interest. (vi) The dividing streamline separates from the body at the trailing edge.

Two different approaches will be pursued and the results compared in an attempt to isolate the effects of upstream influence. In the first approach, one neglects upstream influence and assumes separation to occur at the trailing edge, but relaxes simplifying assumptions (ii) to (v). The procedure is similar to Goldstein's flat plate trailing edge solution in that we seek a locally valid series solution in the right half plane which satisfies a Blasius boundary-layer profile at separation. The basic differences are that we employ the full incompressible Navier–Stokes equation, satisfy the non-slip condition at the rear wall, place no restrictions on the pressure field in advance, and allow a non-zero initial inclination angle for the dividing streamline. In the second approach we relax, in addition, simplifying assumptions (i) and (vi) and seek a Stokes flow solution about the trailing edge that is based on the analysis presented in §§2–4. The arbitrary constants appearing in the solution are left unspecified. Instead, one parametrically varies these constants to see how they influence the location and shape of the separation streamline.

No upstream influence

The x and y co-ordinates have their origin at the trailing edge, and are taken perpendicular and parallel to the rear wall respectively, which is assumed perpendicular to the upper surface of the body (see figure 6). The boundary conditions at $x = 0$ are that the initial profiles for the velocity components can be expressed as an infinite series in integer powers of y for $y > 0$ (the Blasius profile is just a

special case of this series), and that all velocities vanish for $y < 0$. Thus, we write

$$u = 0, \quad v = -\sum_{i=1}^{\infty} a_i r^i \quad \text{for} \quad x = 0, \quad y > 0, \tag{6.1}$$

and

$$u = v = 0 \quad \text{for} \quad x = 0, y < 0. \tag{6.2}$$

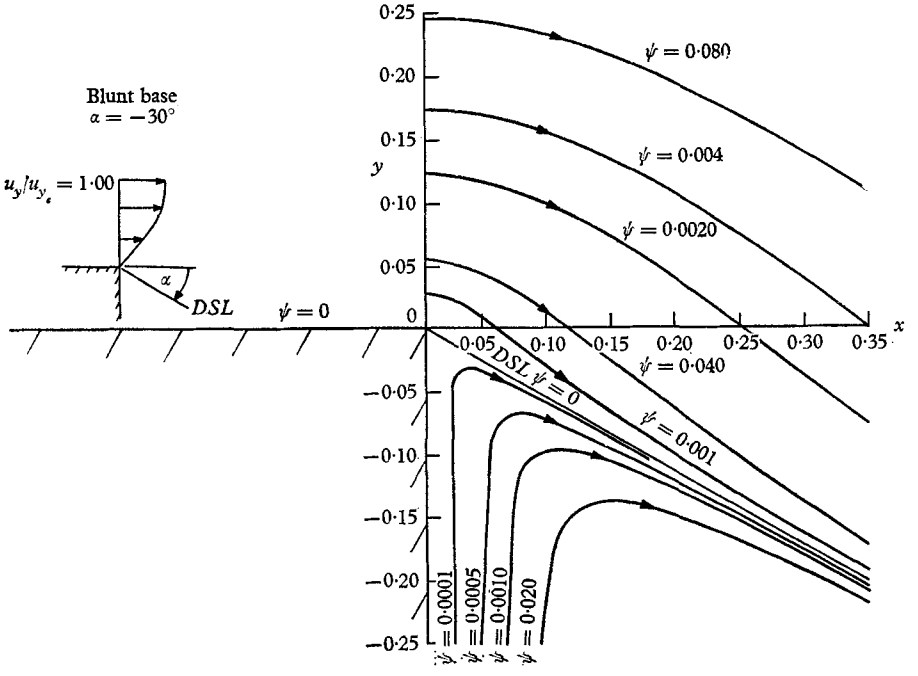

FIGURE 6. Zeroth-order solution equation (6.4) for blunt-based trailing edge with no upstream influence.

The dividing streamline $\psi = 0$ separates from the trailing edge with an initial inclination angle α,

$$\psi = 0 \quad \text{at} \quad \theta = \alpha \quad \text{as} \quad r \to 0, \tag{6.3}$$

which is determined by the expansion to the base pressure of the streamlines in the lower portion of the boundary layer.

The separation point boundary value problem is then to develop a series solution to (2.6) in the right half-plane which satisfies the boundary conditions (6.1), (6.2) and (6.3). One method of treating this boundary value problem is to generalize suitably the classical analysis developed by Goldstein (1930) for the flat plate trailing edge. One introduces the transformed co-ordinates $\xi = f(x)$ and $\eta = y/f(x)$ and seeks a series solution of the form

$$\psi = g(\xi) \sum_{i=0}^{\infty} \phi_i(\eta) \xi^i.$$

This approach is pursued by the author in Weinbaum (1966*a*). In the Goldstein flat plate trailing edge analysis, the lowest order balance is between inertial and viscous forces. $f = x^{\frac{1}{3}}$, $g = x^{\frac{2}{3}}$ and the governing equation for $\phi_0(\eta)$ is non-linear

and must be solved numerically. In the present theory u and v are of the same order of magnitude near the trailing edge, and the lowest order force balance near $r = 0$ is between viscous and pressure forces. $f = x$, $g = x^2$ and the governing equation for $\phi_0(\eta)$ is linear and can be solved analytically. However, one can show that this equation for $\phi_0(\eta)$ is equivalent to (2.7), and that the solution of interest is the case $m = 2$, equation (2.9*b*). The boundary conditions (6.1), (6.2) and (6.3) determine the constants A_i. This solution for the leading term in the series solution for ψ is

$$\psi^{(0)} = \frac{a_1}{4\pi} r^2\{\sin 2\theta + 2\theta + \pi - [(\pi + 2\alpha)\sec^2\alpha + 2\tan\alpha]\cos^2\theta\}, \tag{6.4}$$

where $a_1 = (\partial u_x/\partial y)|_{x=0}$ is the wall shear at the trailing edge.

In figure 6 we have plotted equation (6.4) for $a_1 = 0{\cdot}66412$, the value of a_1 corresponding to the Blasius flat plate solution, and $\alpha = -30$ degrees. To lowest order, the dividing streamline is a straight line. Within the framework of this simplified model, the shearing stress induced on the rear wall by the motion of the fluid above the dividing streamline is independent of y

$$\left.\frac{\partial u_y}{\partial x}\right|_{x=0} = \frac{a_1}{2}\left\{1 + \frac{2}{\pi}\left[\left(\alpha + \frac{\pi}{2}\right)\tan^2\alpha + \tan\alpha + \alpha\right]\right\}. \tag{6.5}$$

Therefore, the ratio σ of the wall shear on the upper surface at the separation point, $\partial u_x/\partial y|_{x=0} = a_1$, to that on the rear wall, (6.5), depends only on the initial inclination angle of the dividing streamline when one neglects upstream influence. Some representative values of σ are given below:

α (*degrees*)	0	-10	-20	-30	-40	-50	-60	-70
σ	2·0	2·4867	3·0807	3·8358	4·8473	6·3092	8·6655	13·2626

These results suggest that the initial inclination angle of the dividing streamline is significant in the angular momentum balance for the recirculating flow. This effect is neglected in present boundar-layer type mixing analyses.

Upstream influence

In the foregoing analysis, the effect of the upstream influence on the pressure field across the corner was purposely omitted. One can easily show that one of the major shortcomings of the solution (6.4) is just the fact that the pressure field corresponding to this solution cannot be matched with the uniform pressure field of the Blasius solution at $x = 0$, for $y > 0$. For $x = 0$ and $y < 0$, the rear wall, the pressure falls monotonically with distance from the corner. If one accepts the premise that the pressure field in the vicinity of the corner is qualitatively similar for a subsonic and supersonic blunt-based trailing edge, then the pressure distribution along the rear wall predicted by (6.4) is also suspect since it is just the opposite trend from Hama's measurements mentioned earlier.

Returning to figure 4, one sees that there are only two roots which satisfy (3.2*a*) and (3.2*b*) when $\theta_0 = \frac{3}{4}\pi$. These roots, $m_1 = 1{\cdot}544$ and $m_2 = 1{\cdot}909$, correspond to the antisymmetric and symmetric flow solutions in that order. In contrast to the $\theta_0 = \frac{1}{2}\pi$ and π cases where there are an infinite multiplicity of slow

motion eigenvalues to choose from, there is no ambiguity when $\theta_0 = \frac{3}{4}\pi$. From (3.3), the two leading terms for $\psi^{(0)}$ are

$$\psi^{(0)} = A_1 r^{m_1}[\cos m_1\theta + \cot\tfrac{1}{4}(3m_1\pi)\cos[(m_1-2)\theta]] + A_2 r^{m_2}[\sin m_2\theta - \tan\tfrac{1}{4}(3m_2\pi)\sin[(m_2-2)\theta]] + \ldots. \quad (6.6)$$

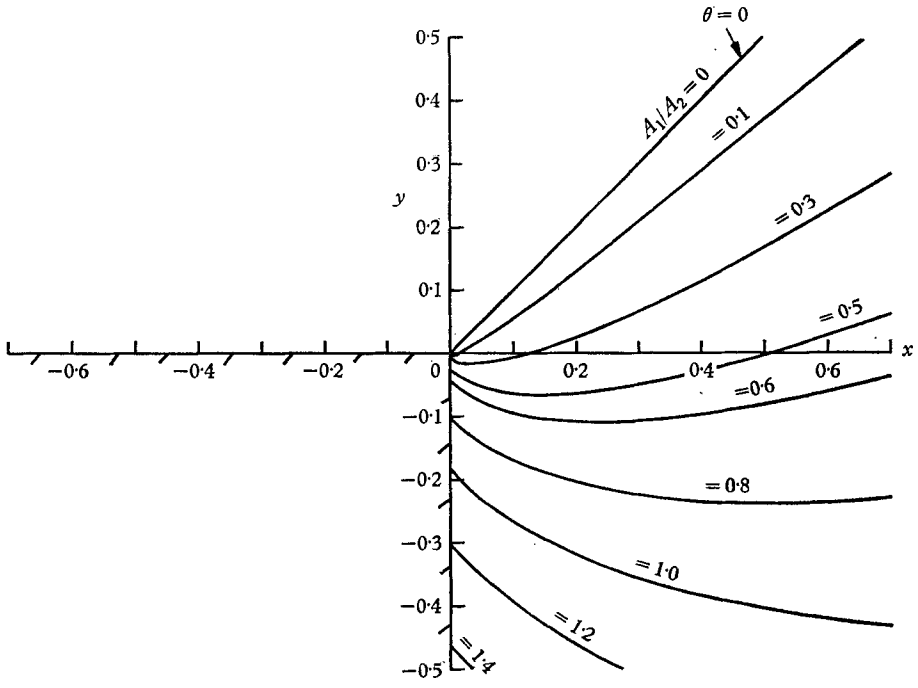

FIGURE 7. Parametric study of the effect of upstream influence on the location and shape of the separation streamline.

The equation of the separation streamline in the vicinity of $r = 0$, for the general case, is obtained by setting $\psi^{(0)} = 0$ in (3.3):

$$r = \left[\frac{-A_1\left(\cos m_1\theta - \dfrac{\cos m_1\theta_0}{\cos[(m_1-2)\theta_0]}\cos[(m_1-2)\theta]\right)}{A_2\left(\sin m_2\theta - \dfrac{\sin m_2\theta_0}{\sin[(m_2-2)\theta_0]}\sin[(m_2-2)\theta]\right)}\right]^{1/(m_2-m_1)}. \quad (6.7)$$

The term in brackets in (6.7) is of 0/0 form at $\theta = -\theta_0$, the rear wall, and to determine the point of separation L'Hopital's rule must be applied twice:

$$r_{\text{separation}} = \left[\frac{-A_1(m_1-1)\cos m_1\theta_0}{A_2(m_2-1)\sin m_2\theta_0}\right]^{1/(m_2-m_1)}. \quad (6.8)$$

In figure 7, equation (6.7) has been plotted with the ratio A_1/A_2 as a parameter, for the case $\theta_0 = \frac{3}{4}\pi$. The spectrum of possible separation streamline shapes is shown in the figure. The ratio A_1/A_2 is a measure of the varying amounts of the symmetric and antisymmetric components present in the solution. Starting with

$A_1 = 0$, the purely symmetric solution, one finds that the direction of the separation streamline turns toward the axis and the separation point moves away from the trailing edge along the rear wall as increasing amounts of the antisymmetric solution are added.† Thus, separation cannot occur at the trailing edge for a wall with zero slip if the energy input at large distances is not symmetric. The angle at which the separation streamline leaves the wall is readily determined. The angle β between the radius vector and the tangent to the separation streamline is given by

$$\tan\beta(\theta) = \frac{r\,d\theta}{dr} = (m_2 - m_1)\frac{f_1 f_2}{f_2 f_1' - f_1 f_2'}, \tag{6.9}$$

where the equation of this streamline (6.7) has been written in the compact form $0 = r^{m_1} f_1(\theta) + r^{m_2} f_2(\theta)$. At $\theta = -\theta_0$, the rear wall, equation (6.9) is of 0/0 form, since $f_1(-\theta_0) = f_1'(-\theta_0) = 0$. However, $\beta(-\theta_0)$ the flow separation angle can be determined through the repeated application of L'Hopital's rule. This result is

$$\cot\beta(-\theta_0) = -\frac{1}{12}\left(\frac{1}{m_2 - m_1}\right)\left[\frac{m_1^3 \sin m_1\theta_0 - (m_1-2)^3(\cos m_1\theta_0)\tan[(m_1-2)\theta_0]}{(m_1-1)\cos m_1\theta_0}\right.$$
$$\left. + \frac{m_2^3 \cos m_2\theta_0 - (m_2-2)^3(\sin m_2\theta_0)\cot[(m_2-2)\theta_0]}{(m_2-1)\sin m_2\theta_0}\right]. \tag{6.10}$$

The interesting observation is that $\beta(-\theta_0)$ is independent of the coefficients A_1 and A_2.‡ Thus, the flow separation angle depends only on the wedge geometry or the angle θ_0. One can show from equation (6.10) that $\beta(-\theta_0)$ decreases monotonically from a maximum of 90 degrees when $\theta_0 = \frac{1}{2}\pi$ to zero degrees when $\theta_0 = \pi$, and that for $\theta_0 = \frac{3}{4}\pi$, $\beta \approx 41{\cdot}2$ degrees.

A related problem of much interest is the separation condition at the trailing edge of a sharp edged airfoil. For thin airfoils at small incidence, it is an empirical observation that separation always occurs very close to the trailing edge, the Kutta condition. In the inviscid theory, this condition is necessary to determine uniquely the circulation about the body. To study the viscous separation condition that exists in a real fluid, the analysis just described for the blunt-based trailing edge was repeated for a 5-degree half angle trailing edge typical of a thin airfoil, $\theta_0 = 175$ degrees. It was found that to displace the separation point more than a Stokes radius from the trailing edge, the asymmetry ratio A_1/A_2 had to exceed ≈ 8. Since A_1 and A_2 are directly related to the external flow above and below the airfoil, this suggests that significant asymmetries in the external flow are required to displace the separation point more than the characteristic viscous length from the trailing edge. Thus, the viscous forces near the trailing edge, although they act locally, can provide a very important constraint on the overall motion.

† The Reynolds number dependence of the coefficients A_1 and A_2 enters through the coupling with the inviscid outer flow. Roache's (1967) numerical results suggest that the ratio A_1/A_2 increases, and hence the separation point moves down on the base, as Re_∞ decreases. In the limit as $Re_\infty \to \infty$ separation occurs infinitesimally close to the corner, whereas for the opposite limit $Re_\infty \to 0$ separation occurs at the base stagnation point.

‡ H. E. Topakoglu independently discovered this result and reported it to the author in a private communication.

The pressure field in the neighbourhood of the corner is readily derived from (2.2), (2.3) and (3.3):

$$p = 4(m_1-1)A_1\left(\frac{\cos m_1\theta_0}{\cos[(m_1-2)\theta_0]}\right)r^{m_1-2}\sin[(m_1-2)\theta] - 4(m_2-1)A_2\left(\frac{\sin m_2\theta_0}{\sin[(m_2-2)\theta_0]}\right)r^{m_2-2}\cos[(m_2-2)\theta] + \text{const.} + O(r^{2m_1-2}). \quad (6.11)$$

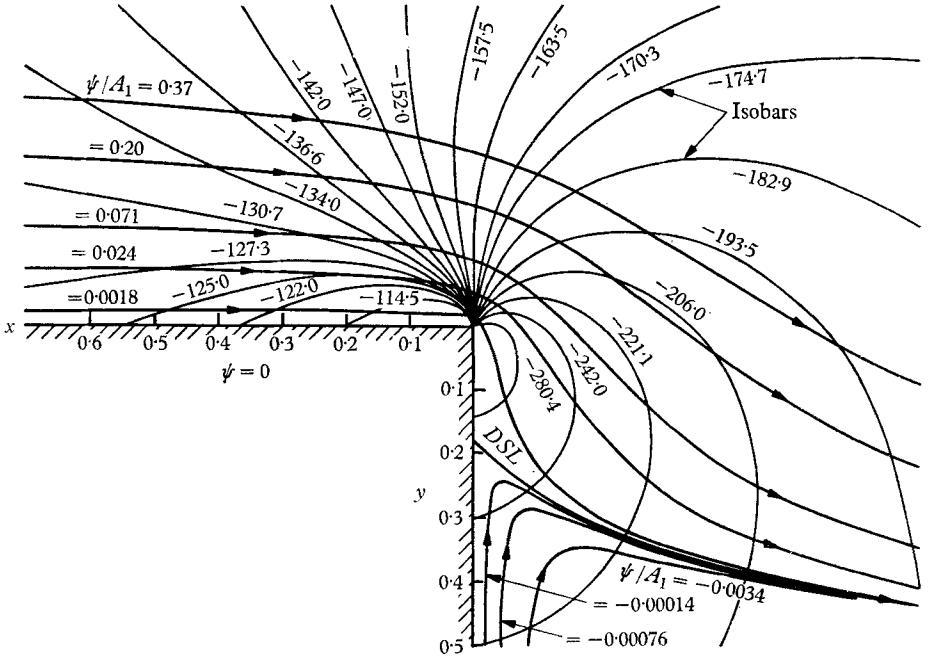

FIGURE 8. Streamline pattern and pressure field in the vicinity of trailing edge, $A_1/A_2 = 1{\cdot}0$.

In figure 8 we have plotted the trailing edge streamline pattern predicted by equation (6.6) for the case $A_1/A_2 = 1$, a situation representative of what one would expect to find in the base flow separation problem. Superimposed are the lines of constant pressure or isobars that obtain from (6.11) when $\theta_0 = \frac{3}{4}\pi$. The pressure scale is arbitrary. Note that the sharp expansion around the corner is followed by a recompression on the rear wall. This adverse pressure gradient causes the flow to separate on the base and suggests that the base pressure is approached asymptotically from below. The theory also predicts a small pressure rise along the upper surface starting roughly one Stokes radius ahead of the corner. From (3.5) one can show that there is a pressure minimum, $p_r = 0$, on the upper surface at

$$r = \left[\frac{A_1(m_1-1)(m_1-2)\cot\frac{1}{4}(3m_1\pi)\cos\frac{1}{4}(3m_1\pi)}{A_2(m_2-1)(m_2-2)\tan\frac{1}{4}(3m\pi_2)\sin\frac{1}{4}(3m_2\pi)}\right]^{1/(m_2-m_1)}. \quad (6.12)$$

For $A_1/A_2 = 1$, this pressure minimum occurs at $r \approx 1{\cdot}2$; $p = -127{\cdot}0$ at this point using the scale shown in figure 8. Preceding this minimum, p falls mono-

tonically as one approaches the corner starting several boundary-layer thicknesses ahead of the corner. The major portion of the pressure drop across the corner occurs in a distance that is small compared to the Stokes radius. Therefore, as one might expect, the pressure is 'weakly singular' at $r = 0$ in the terminology of Lugt & Schwiderski. The shear at the trailing edge is finite rather than zero as some investigators have suggested. The separation on the rear wall seems necessary to avoid the discontinuity in shear that would have resulted had separation occurred at the trailing edge and the shear not been zero. Finally, the separation point behaviour just described is in qualitative agreement with Hama's experiments.

To summarize briefly the results in this section, upstream influence produces the following changes in the flow near the trailing edge of a blunt-based body: (i) the separation point is dislodged from the trailing edge if there is any asymmetry in the external flow, (ii) the separation streamline is not a straight line but has a significant curvature near the separation point, (iii) the separation angle depends only on the wedge angle and is independent of the external flow, (iv) the flow undergoes a compression along the rear wall beneath the corner so that the base pressure is approached from below, (v) a 'weak singularity' in the pressure field is admissible at $r = 0$ to allow for the sharp drop in pressure across the corner that occurs on the microscopic length scale, and (vi) the shear is both finite and continuous at the trailing edge.

7. The supersonic trailing edge

In this section, the foregoing insights into the behaviour of the viscous underlayer will be combined with our existing knowledge of the rotational expansion that takes place in the supersonic portion of the boundary layer to provide a complete qualitative description of the expansion and separation process that occurs at the shoulder of a supersonic blunt based body. As mentioned in the introduction, the wave interaction theory by itself predicts results that differ in several important respects with Hama's (1967) recent experiments. The principal differences are the fact that the lip shock wave forms much closer to the corner than the wave interaction theory predicts and that the flow does not expand monotonically to the base pressure but experiences a recompression beneath the corner on the rear wall, the base pressure being approached from below. Theory and experiment suggest that two closely related phenomena are present, the separation from the base wall and the coalescence of Mach waves from the constant pressure base region. The detailed coupling of these two phenomena is schematically shown in figure 9, and is described below.

The primary expansion of the supersonic flow starts at some point slightly upstream of the corner. Primary expansion waves have large curvature because of the Mach number gradient in the boundary layer. The centre of the primary expansion fan, therefore, appears to be located at some point d that is of the order of a boundary-layer thickness ahead of the corner. This effect is visible in figure 2 and was noted by Hama. The linearized wave theory in Weinbaum (1966*b*) shows that when $M > \sqrt{2}$ the strength of a Mach wave is significantly augmented as it propagates through the higher Mach number regions of the boundary layer into

the outer flow. Thus, the streamline at the outer edge of the boundary layer experiences a sizeably greater drop in pressure than a streamline near the sonic line when both streamlines have traversed the same primary waves. It has been well documented by Hama and others that the pressure drop across the free

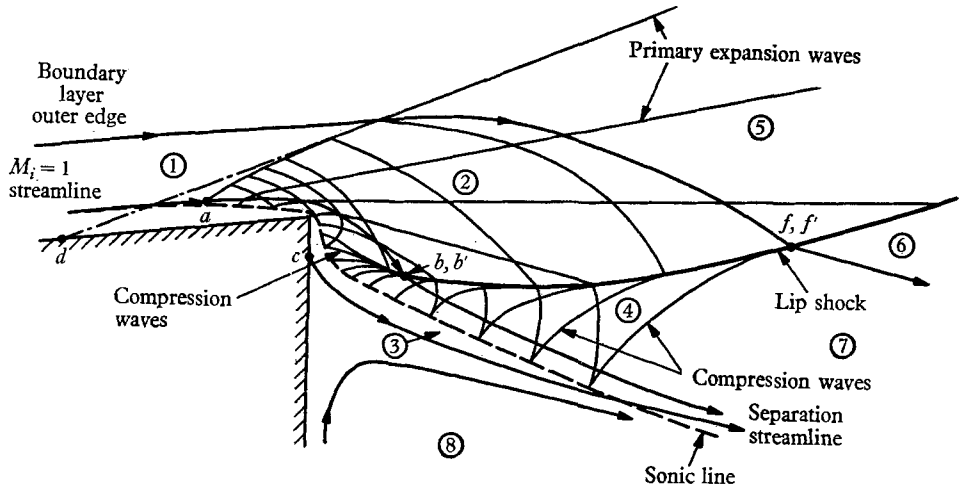

FIGURE 9. Schematic diagram of the separation and expansion of a supersonic boundary layer at a blunt-based trailing edge.

shear layer in the region downstream of the intersection of the lip shock and the outer edge of the free shear layer point f is rather small. Regions (6), (7) and (8) are, therefore, at essentially the same pressure, the base pressure p_8. Let b and f denote conditions just ahead of the lip shock and b' and f' conditions just behind it. The lip shock must increase in strength between points b and f, for the overexpansion at f is greater than that at b, while the pressure at points b' and f' are both nearly equal to the base pressure. Region (4) is a region of reflected wave interaction in which the strength of the lip shock gradually adjusts so that by the time the lip shock emerges from the shear layer at point f its strength is just sufficient to recompress the overexpanded inviscid outer flow back to the base pressure. The lip shock in regions (2) and (5) is thus the corrective recompression needed to balance the initial overexpansion of the outer supersonic portion of the boundary layer and the inviscid flow.

The theory in Weinbaum (1966*b*) and Weiss & Weinbaum (1966) treats the line abb' as a single point, and therefore, incorrectly treats the incipient formation of the lip shock. However, downstream of point b', the rotational characteristic calculation performed in the above investigations does employ a boundary condition that is eventually achieved by the actual flow, namely that the $M_i = 1$ streamline approaches the measured base pressure. For small distances from the corner, the rotational characteristics solution is very poor (the compression waves from the $M = 1$ surface have not yet had a chance to coalesce, whereas for the real flow the toe of the lip shock has already formed), while if one proceeds further from the corner toward the outer portions of regions (2) and (4) the description

of the rotational characteristic solution rapidly improves. It is for this reason that the asymptotic strength and direction of the lip shock as predicted by the characteristic calculation shown in figure 1 of Weiss & Weinbaum (1966) agrees favourably with the experiment on which it was based (Larson, Scott, Elgin & Siever 1962).

The essentially inviscid motion in the supersonic portion of the boundary layer, just described, is coupled to the viscous motion in the subsonic underlayer through the interaction between the growth of the displacement thickness of the subsonic layer and the induced pressure field in the supersonic region. In negotiating the corner, the subsonic flow encounters an adverse pressure gradient on the base wall, see figure 8, which produces first a rapid increase in displacement thickness of the viscous underlayer and then separation. These compression waves propagate through region 3 in figure 9 into the supersonic flow in region 4 where they coalesce to form the lip shock wave. Having turned the corner, the flow is directed toward the wake centreline and a recompression is required to turn the flow back to the free stream direction. While this recompression is strongest in the vicinity of the wake reattachment stagnation point its effects are readily communicated upstream through the low speed flow in regions 3 and 8. It is this upstream influence that initiates the interaction on the base wall and leads to separation.

8. The near wake rear stagnation point

We next look at the reattachment stagnation point formed by the symmetric rejoining of two laminar viscous layers. This solution is developed both in rectangular Cartesian co-ordinates Cheng (1964) and in polar co-ordinates (Weinbaum 1966*a*).† Of particular interest here is the derivation of the closure condition described at the end of §1. Since all velocities become vanishingly small as the stagnation point is approached, one expects that a Stokes type expansion is valid in the stagnation region. The only local boundary and auxiliary conditions applicable are that a stagnation point and symmetry plane exist. Thus,

$$\left.\begin{aligned} &u = v = 0 \quad \text{at} \quad r = 0, \\ \text{and} \quad &\psi = \psi_{\theta\theta} = 0 \quad \text{at} \quad \theta = 0 \text{ and } \pi. \end{aligned}\right\} \tag{8.1}$$

One can show that the only solutions to the biharmonic equation (2.7) which satisfy (8.1) are of the form

$$\psi_1^{(0)} = r^m(A_1 \sin m\theta + A_2 \sin (m-2)\theta), \tag{8.2}$$

where $m = 2, 3, 4, \ldots$, etc. For the lowest root $m = 2$, $A_2 = 0$. The $m = 2$ term is irrotational and, therefore, does not contribute by itself to the non-linear part of the vorticity equation (2.6). Thus, the first three terms in the expansion for ψ are

$$\psi = A_1 r^2 \sin 2\theta + r^3(B_1 \sin 3\theta + B_2 \sin \theta) + r^4(C_1 \sin 4\theta + C_2 \sin 2\theta) + \ldots, \tag{8.3a}$$

or

$$\psi = y[2A_1 x + (3B_1 + B_2)x^2 + (B_2 - B_1)y^2 + 2(2C_1 + C_2)x^3 + 2(C_2 - 2C_1)xy^2] + \ldots, \tag{8.3b}$$

† The reattachment solution is also presented in Reeves & Buss (1967), which appeared subsequent to the writing of this paper.

and to $O(r^4)$ the equation of the dividing streamline *DSL*, the streamline that separates the flow that is turned back along the axis from the flow that passes downstream, is given by

$$A_1 x + \tfrac{1}{2}(3B_1 + B_2)x^2 + \tfrac{1}{2}(B_2 - B_1)y^2 + (2C_1 + C_2)x^3 + (C_2 - 2C_1)xy^2 = 0. \quad (8.4)$$

The slope of this streamline at any station x near $x = 0$ is then

$$\lambda = -\frac{A_1 + (3B_1 + B_2)x + 3(2C_1 + C_2)x^2 + (C_2 - 2C_1)y^2}{(B_2 - B_1)y + 2(C_2 - 2C_1)xy}. \quad (8.5)$$

Therefore, as previously deduced by Cheng (1964), λ is infinite at the origin or the *DSL* stagnates perpendicular to the axis provided $A_1 \neq 0$. The case $A_1 = 0$, while it does correspond to a finite slope, cannot represent the near wake stagnation point. The axial velocity does not change sign at the stagnation point so that the *DSL* approaches $r = 0$ with slope $-\lambda$ and leaves with slope $+\lambda$.

Of primary interest is the coupling between the forward and reverse flow velocities at the end of the recirculation region. In particular, one wishes to know how q^*, the magnitude of the velocity on the *DSL*, and q_0, the magnitude of the velocity on the wake centreline, are related at a given x station near the stagnation point. The slope of the *DSL*

$$\lambda = u_y^*/u_x^* = -\psi_x^*/\psi_y^*, \quad (8.6)$$

so that by definition

$$q^* = (\lambda^2 + 1)^{\frac{1}{2}}\psi_y^*, \quad (8.7)$$

where the asterisk denotes conditions on the *DSL*. Combining (8.3*b*), (8.4) and (8.7), one finds that

$$q^*(x) = -2(\lambda^2 + 1)^{\frac{1}{2}}[2A_1 x + (3B_1 + B_2)x^2 + 2(2C_1 + C_2)x^3]. \quad (8.8)$$

The velocity on the centreline from (8.3*b*) is given by

$$q_0(x) = 2A_1 x + (3B_1 + B_2)x^2 + 2(2C_1 + C_2)x^3. \quad (8.9)$$

q_0 is, therefore, simply the term in brackets in (8.8). Hence,

$$\left(\frac{q_0(x)}{q^*(x)}\right)^2 = \frac{1}{4(\lambda^2(x) + 1)}. \quad (8.10)$$

Thus, there is a unique relationship between λ, q^* and q_0 in the Stokes region, region I in figure 10, that must be obeyed if the wake is too close. q_0/q^* increases monotonically from zero at $r = 0$ to some value corresponding to the asymptotic direction of the *DSL* at the edge of region I (see figure 10). It is not clear how to interpret the condition imposed by (8.10). Like the Kutta condition at the trailing edge of an airfoil, (8.10) is independent of the external flow. This condition could, for example, affect the vorticity in the interior of the recirculation region since the velocity coupling at the reattachment point may be important in determining the circulation on the $\psi = 0$ streamline that bounds the recirculation region. Suppose one formulates the recirculation region as an initial value problem in which one prescribes the shape of and the velocity distribution along the *DSL*, and proceeds downstream toward region I in figure 10 using a suitable marching technique. The unknown initial conditions in such a procedure are

the reference pressure p_b, the pressure gradient $p_y(0, y)$, and the shear $v_x(0, y)$ on the base wall. In such improperly posed initial value problems, the question of uniqueness and the stability of the numerical solution are closely related. With $p_y(0, y)$ and $v_x(0, y)$ specified, the numerical marching procedure will yield some

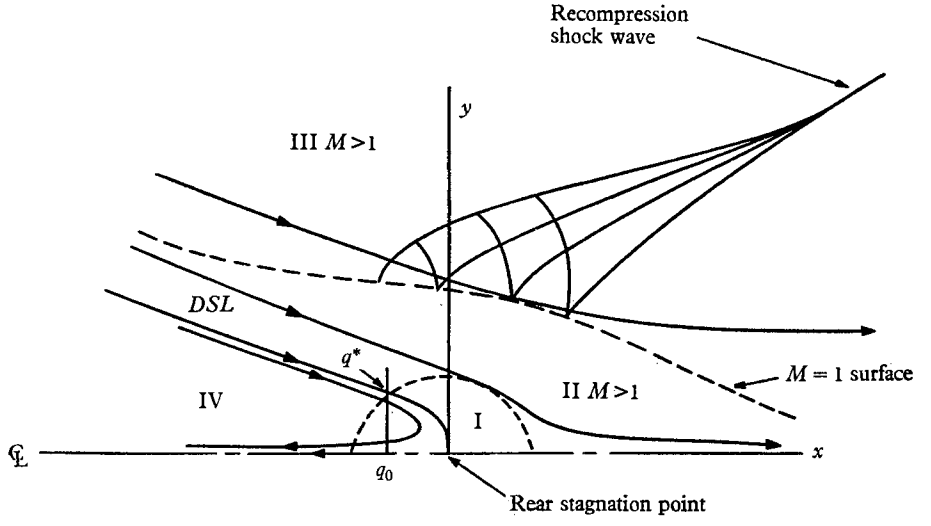

FIGURE 10. Wake reattachment, $A_1 \neq 0$.

value of the ratio q_0/q^* as the *DSL* approaches the centreline. However, it would seem that unless these initial conditions were chosen correctly, (8.10) will not be satisfied and the wake will not close, and that unless p_b is correct the flow will not pass through the downstream throat predicted by the Crocco-Lees (1952) theory.† These hypotheses are currently being studied further.

The author wishes to thank Dr Richard W. Garvine for numerous fruitful discussions of this material and for reading and usefully commenting on the final manuscript.

A preliminary version of this paper was given as an invited talk 'Laminar leading and trailing edge flows and the near wake rear stagnation point' at the AGARD Specialists Meeting on 'Separated flows' at the von Kármán Institute for Fluid Dynamics 10–13 May 1966, and is available as General Electric TIS Report R 66 SD 25. The author wishes to acknowledge the support of the General Electric Space Sciences Laboratory, King of Prussia, Pennsylvania, under whose sponsorship much of this work was done.

† The throat for a two-dimensional viscous layer is simply the station for which the integral

$$\int_0^\delta \frac{M^2-1}{M^2}\,dy$$

across the layer vanishes (see Weinbaum 1967).

REFERENCES

CARRIER, G. F. & LIN, C. C. 1948 *Q. Appl. Math.* **6**, 63.

CHENG, S. I. 1964 *Princeton University Dept. of Aerospace and Mechanics Rept.* no. 701.

CROCCO, L. & LEES, L. 1952 *J. Aero. Sci.* **19**, 649.

DENISON, M. R. & BAUM, E. 1963 *A.I.A.A. J.* **1**, 342.

DEAN, W. R. & MONTAGNON, P. E. 1949 *Proc. Camb. Phil. Soc.* **45**, 389.

DONALDSON, I. S. 1967 *A.I.A.A. J.* **5**, 1086.

GOLDSTEIN, S. 1930 *Proc. Camb. Phil. Soc.* **26**, 1.

HAMA, F. R. 1967 *A.I.A.A. Preprint*, no. 67–29.

HARPER, J. F. 1963 *J. Fluid Mech.* **17**, 141.

HOWARTH, L. 1934 *Rept. Memor. Aero. Res. Coun., Lond.* no. 1632.

KUBOTA, T. & DEWEY, C. F. 1964 *A.I.A.A. J.* **2**, 629.

LARSON, R. E., SCOTT, C., ELGIN, D. & SIEVER, R. 1962 *Univ. Minnesota, Rosemont Aero. Labs. Rept.* no. 183.

LUGT, H. J. & SCHWIDERSKI, E. W. 1965 *Proc. Roy. Soc.* A **285**, 382.

MOFFATT, H. K. 1964 *J. Fluid Mech.* **18**, 1.

REEVES, B. L. & BUSS, H. 1967 *A.I.A.A. Preprint*, no. 67–64.

ROACHE, P. J. 1967 Ph.D. thesis, University of Notre Dame, Notre Dame, Indiana.

VIVIAND, H. & BERGER, S. A. 1965 *J. Fluid Mech.* **23**, 439.

WEINBAUM, S. 1966*a* *General Electric TIS Rept.* R 66 SD 25.

WEINBAUM, S. 1966*b* *A.I.A.A. J.* **4**, 217.

WEINBAUM, S. 1967 *A.I.A.A. Preprint*, no. 67–65.

WEISS, R. F. & WEINBAUM, S. 1966 *A.I.A.A. J.* **4**, 1321.

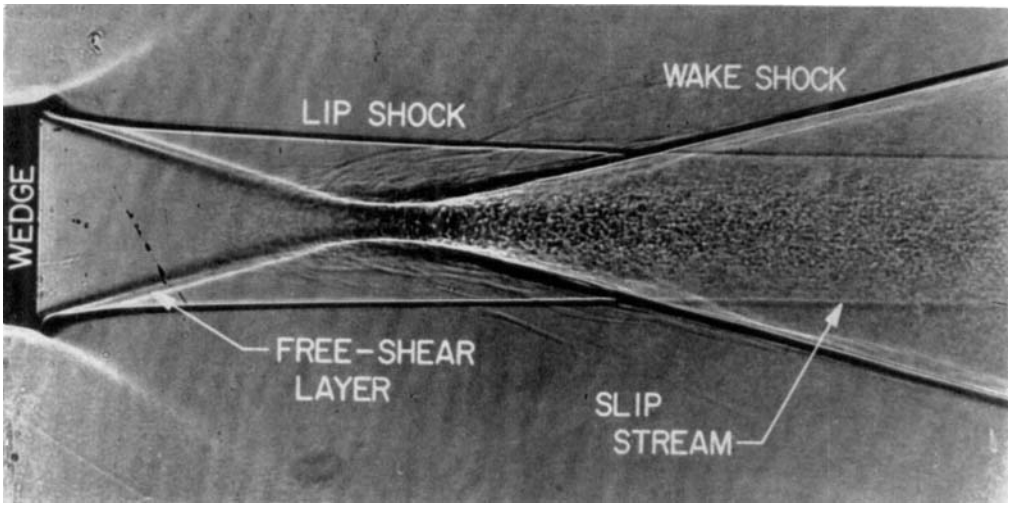

FIGURE 2. Shadowgraph of flow behind a wedge, $M_\infty = 2{\cdot}61$, $\mathrm{Re}_{\infty L} = 1{\cdot}01 \times 10^6$, courtesy of F. R. Hama (1967).